MATHEMATICAL MODELLING FOR EXPERIMENTAL ARCHAEOLOGY: CASE STUDIES FOR MECHANICAL TOOLS IN HALLSTATT SALT MINES

Bernhard Heinzl[(a)], Erik Auer[(b)], Benedikt Slowacki[(c)], Kerstin Kowarik[(d)], Hans Reschreiter[(e)], Niki Popper[(f)], Felix Breitenecker[(g)],

[(a) (b) (c) (g)]Institute for Analysis and Scientific Computing, Vienna University of Technology
[(d) (e)]Natural History Museum Vienna, Austria
[(a) (f)]dwh Simulation Services, Vienna

[(a)]bernhard.heinzl@tuwien.ac.at, [(b)]e0926305@student.tuwien.ac.at, [(c)]e0825658@student.tuwien.ac.at, [(d)]kerstin.kowarik@nhm-wien.ac.at, [(e)]hans.reschreiter@nhm-wien.ac.at, [(f)]niki.popper@drahtwarenhandlung.at, [(g)]felix.breitenecker@tuwien.ac.at,

ABSTRACT
In a cooperative project between the Natural History Museum Vienna and the Vienna University of Technology, students are assigned a variety of tasks in modelling and simulation of physical systems. These systems originate from archaeological investigations on the prehistoric salt mines in Hallstatt (Austria) in the Bronze Age. The first example studies different designs of rope pull systems used to hoist the broken salt from the mining halls through shafts to the surface. In the second task, bronze picks for breaking the salt are investigated. The third and last task presents some calculations regarding illumination and air consumption in the mining halls. The calculations and simulation results help archaeologists gain knowledge about the working conditions and technical equipment in the prehistoric salt mines. For the students, the provided examples give interesting insights into practical applications of modelling and simulation.

Keywords: mechanical systems, teaching, mathematical modelling, archaeology

1. INTRODUCTION
The prehistoric salt mines of Hallstatt in Austria are subject of great interest for archaeologists. Salt mining activities are dated to 1458-1245 B.C. in the Bronze Age (Grabner et al. 2006).

A large amount of archaeological finds of technical equipment and organic materials (timber, wooden tools, strings of bast, fur etc.) and the perfect conditions of preservation in the mines due to the conserving properties of salt allow for a reconstruction of the working process in the mines (Reschreiter et al. 2009).

These investigations suggest that mining was organized in an efficient, nearly industrial manner with highly specialized tools. Salt was mined in underground mining chambers using special bronze picks. The resulting small pieces of salt were then collected in buckets and transported to the vertical shaft where it was hoisted to the surface using a wool sack or cloth attached to a linden bast rope (Kowarik et al. 2012).

The high degree of specialization and functionality observable on certain tools and the design for high efficiency suggest that the workforce had highly specialized knowledge in mining technology and infrastructural processes (Kowarik et al. 2012).

Typically, experimental methods using reconstructions of historical technologies are used in archaeology to provide deeper insights on technological issues. As a new tool, modeling and simulation can also serve as a method for gaining knowledge in different aspects of archaeology.

As part of a collaboration between the Natural History Museum Vienna and the Vienna University of Technology, certain tasks are defined, which were assigned to students as part of their basic training in modelling and simulation. The obtained results will help archaeologists gain knowledge about tools and working processes in the prehistoric salt mines in Hallstatt for a technological reconstruction.

The following sections give a brief description of some current tasks, which investigate certain aspects of the mining process.

2. ROPE PULL SYSTEMS
Rope pull systems were used to hoist the broken salt from the mining halls through shafts to the surface (see figure 1). While there are archaeological findings of bast ropes and other appliances, there are still some matters regarding the construction, length and arrangement of the rope pull systems at issue.

To estimate and compare the time and strength requirements for transporting the salt, various options are investigated using simulation models. For example we compare two variants of the rope design, an open and a closed version, depicted in figure 2. In the closed version, both ends of the rope are connected which enables more uniform distribution of the rope mass and therefore less requirement for external forces. An important issue also concerns modelling of the rope guide, for which we consider two possibilities, one with sliding friction on a log and one with return pulley.

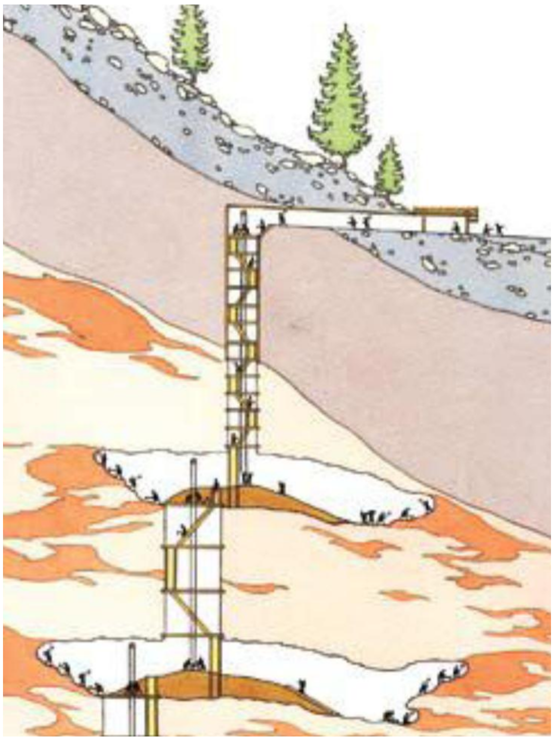

Figure 1: Schematic Reconstruction of the Excavation Chambers and Shaft Structure with Rope Pull Systems (© D. Gröbner, H. Reschreiter, NHM Vienna)

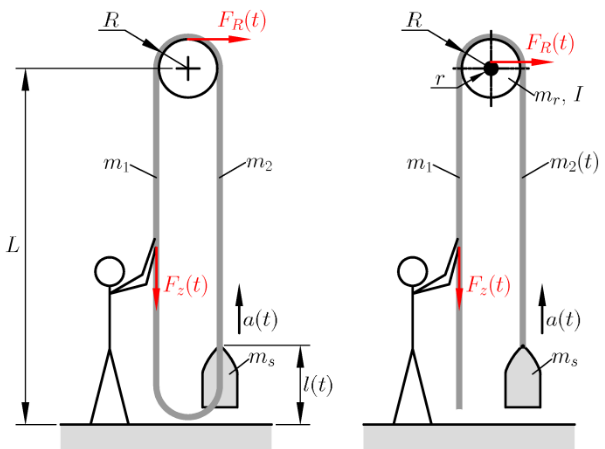

Figure 2: Different Design Options with Closed Rope (Left) or Open Rope (Right) for the Rope Pull System. The Schematic also Shows Two Possibilities for the Rope Guide: Sliding Friction on a Log (Left) and Rotating Return Pulley (Right).

2.1. Rope deflection on a log

Considering simple balance of forces according to figure 2 taking into account mass of the rope on both sides (m_1 and m_2, resp.) and forces of inertia leads to the following equation:

$$F_z(t) + m_1(g - \mathrm{a}(t)) - F_R(t) = m_2(t)\big(g + a(t)\big) + m_s\big(g + a(t)\big), \qquad (1)$$

with external force $F_z(t)$, predefined acceleration $a(t)$ (see equation (4)), acceleration of gravity g and mass of the salt bags m_s. The coulomb friction force $F_R(t)$ is defined as

$$F_R(t) = \mu(v(t))[F_z(t) + m_1\big(g - a(t)\big) + m_2(t)\big(g + a(t)\big) + m_s\big(g + a(t)\big)]. \qquad (2)$$

The expression in square brackets denotes the total normal force on the log. For the friction coefficient μ, we define the following expression depending on the rope velocity v, also visualized in figure 3:

$$\mu(v) = (\mu_c + (\mu_{\mathrm{brk}} - \mu_c)\exp(-c_v|v|)\,\mathrm{sgn}(v) + fv, (3)$$

with a coulomb friction coefficient μ_c, breakaway friction coefficient μ_{brk}, viscous friction coefficient f and coefficient c_v. This friction model takes into account sticking friction at velocities near zero (μ_{brk}) as well as viscous friction at high velocities (fv).

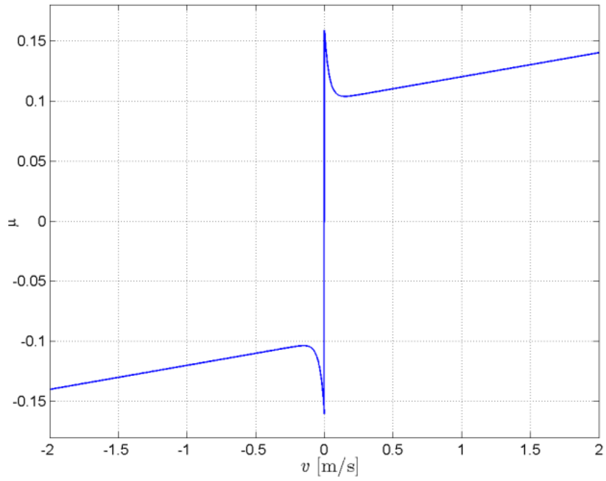

Figure 3: Model of the Friction Coefficient μ with Sticking and Viscous Components for Parameters $\mu_c = 0.1$, $\mu_{\mathrm{brk}} = 0.16$, $c_v = 30$ and $f = 1/50$.

In order to determine the forces necessary for hoisting the salt to the surface, the proposed model receives the desired velocity over time as input signal and calculates the necessary external force $F_z(t)$. One possible input signal is depicted in figure 4. It shows a smooth nearly periodic signal with global upward trend.

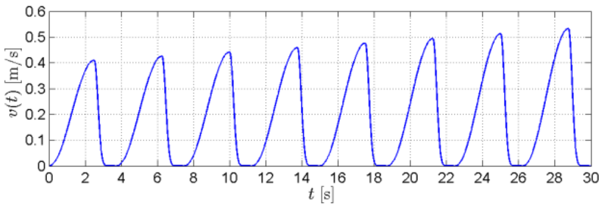

Figure 4: Possible Input Signal $v(t)$ with Smooth Progression and Global Upward Trend.

The external force can then be calculated using equations (1), (2) and (3) and the time derivative

$$a(t) = \frac{d}{dt}v(t) \tag{4}$$

of the input velocity.

For the open rope, the mass $m_2(t)$ of the rope on the right side of the log depends on the current position $l(t)$,

$$m_2(t) = m_{2,0} - \rho l(t), \tag{5}$$

with the assumed density $\rho = 1.5$ kg/m and starting mass $m_{2,0} = \rho L$, and therefore decreases over time according to

$$\frac{d}{dt}m_2(t) = -\rho\frac{d}{dt}l(t) = -\rho v(t) \tag{6}$$

with given input velocity. If the rope is closed (see figure 2 left), then the mass m_2 is constant

$$m_2 = \rho L. \tag{7}$$

In both cases (open and closed rope), the mass m_1 on the left side is assumed constant, also with

$$m_1 = \rho L. \tag{8}$$

The mass of one bag of salt is assumed to be about 28 kg which corresponds to a volume of 20 l. For the value of m_s, one or more bags of salt are considered,

$$m_s = k \cdot 28\,\text{kg}, \qquad k = 1,2,3,\ldots \tag{9}$$

with the number of bags k.

Evaluation of a simulation using the presented equations implemented in MATLAB and parameters $L = 20$ m, $k = 1$ for example for a greased log ($\mu_c = 0.1$, $\mu_{\text{brk}} = 0.16$) provide the results given in figure 5. The results show a total duration of about 81 s to hoist one bag of salt over a height of 20 m, maximum external force is about 500 N. The periodic velocity (see figure 4) leads to a pulsating progression of the height $l(t)$.

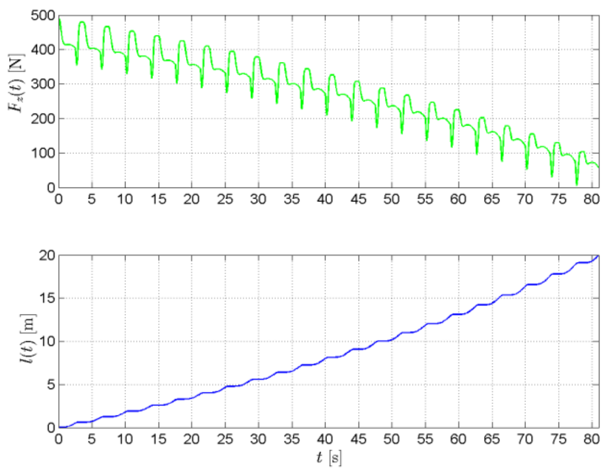

Figure 5: Simulation Results for a Greased Log with Open Rope and $L = 20$ m, $k = 1$.

Similar investigations for different shaft height L as well as different number of bags lead to the results presented in figure 6. It can be seen that each additional bag of salt adds about 400 N to the external force, which is more than the own weight because of additional friction.

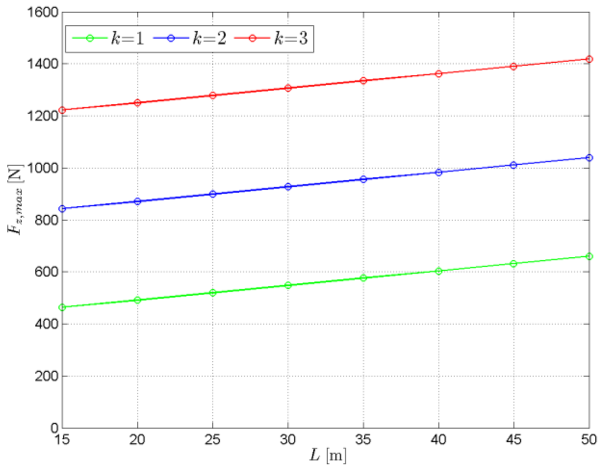

Figure 6: Maximum External Force F_z for the Scenario with Log for Different Shaft Height L and Different Number of Bags k.

2.2. Rope deflection with rotating return pulley

Using a return pulley with outer Radius R and axle radius r instead of a static log adds terms for pulley mass m_r and inertia I to equations (1) and (2), thus, with regard to figure 2, resulting in the new equations

$$F_z(t) + m_1\big(g - \mathrm{a}(t)\big) - F_R(t)\frac{\mathrm{r}}{\mathrm{R}} - \frac{Ia(t)}{\mathrm{R}^2} = m_2(t)\big(g + a(t)\big) + m_s\big(g + a(t)\big), \tag{10}$$

$$F_R(t) = \mu(v(t))[F_z(t) + m_1\big(g - a(t)\big) + m_2(t)\big(g + a(t)\big) + m_s\big(g + a(t)\big) + m_r]. \tag{11}$$

Different values can be considered for the parameters of the pulley depending on its material (wood, bronze, etc.). For a pulley made of wood we get for example the following typical parameters:

$$R = 0.6\text{ m},\ r = 0.2\text{ m},\ m_r = 16.3\text{ kg}, \quad I = 3.3\text{ kgm}^2,\ \mu_c = 0.06,\ \mu_{\text{brk}} = 0.11. \tag{12}$$

As a simulation result, maximum required external force F_z for the scenario with return pulley and different values for shaft height L and number of bags k is presented in figure 7. Comparison with figure 6 shows significant reduced force requirement due to lower friction.

Figure 8 compares Force input between the version with open rope and with closed rope. Since the moving mass is constant for the variant with closed rope, the required force is also constant in average, whereas in the other case the force requirement decreases steadily.

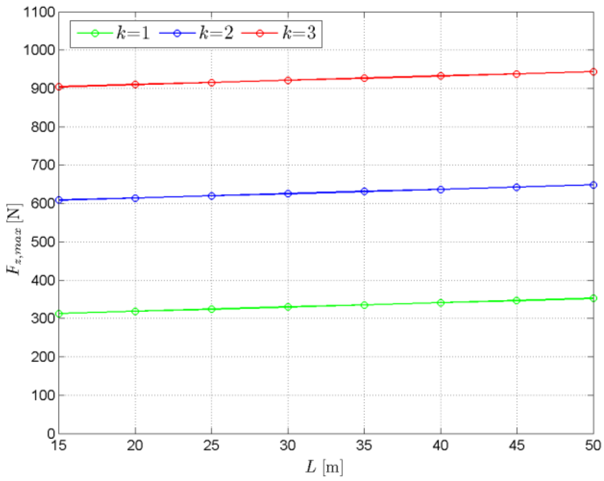

Figure 7: Maximum External Force F_z for the Scenario with Return Pulley for Different Shaft Height L and Different Number of Bags k.

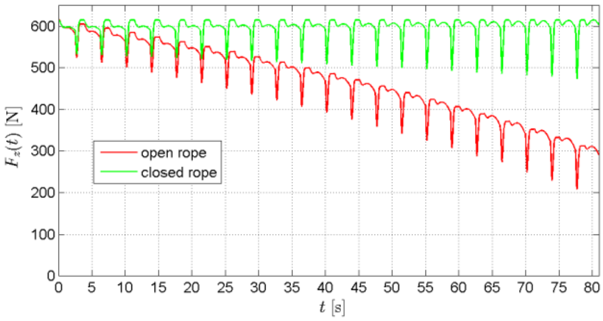

Figure 8: External Force $F_z(t)$ Over Time for the Scenario with Return Pulley and Both Variants of Rope Design.

In summary, it can be said that the simulation results show significant force requirement for the model with sliding friction, especially because of the high mass of the rope. This is also the reason for a limitation regarding the maximum continuous shaft height.

With the presented equations it is also possible to provide the external force $F_z(t)$ and calculate resulting velocity $v(t)$ and position $l(t)$, which will be investigated in further studies.

3. BRONZE PICKS

Salt was mined using bronze picks with wooden handle (see figure 9 left). Highly interesting is the unusual shape of the pick with a typical angle between the shaft and tip of about 55 to 75 degrees. It is believed that this particular shape was adapted to the specific working conditions in the Hallstatt mines, especially since no similar devices have been found at other at archaeological sites. The small angle does not allow typical circular hacking motion, which is why it is not yet completely clear exactly how such a pick was used.

Modelling the pick as a rigid body system (figure 9 right) allows evaluation of possible movement scenarios and comparison regarding resulting force and momentum on the tip.

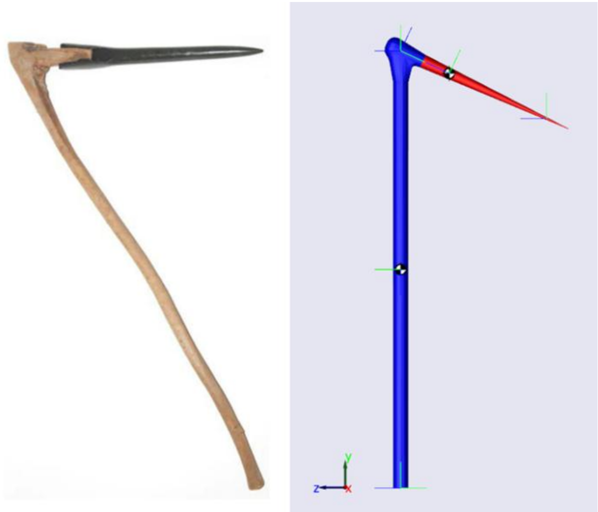

Figure 9: Left: Reconstructed Bronze Age Pick (© A. Rausch, NHM Vienna). Right: Rigid Body Model of the Pick in MATLAB/SimMechanics.

Scenarios of movement are obtained by geometrical considerations, like shown in figure 10. Several points are defined along a trajectory of the tool tip depending on the range of motion for a human. Taking into account the time relation, this trajectory also determines velocity and acceleration behavior. Coordinates for one example trajectory are presented in figure 11. In this figure, impact on the ground occurs at $t = 1$ s. This impact is modeled not as a discontinuous, but as a smoothed transition in velocity.

Special focus is put on the angle, in which the tool tip hits the ground. In order to use the tool effectively, this impact angle is required to be

$$\alpha = 20° \dots 30°. \tag{13}$$

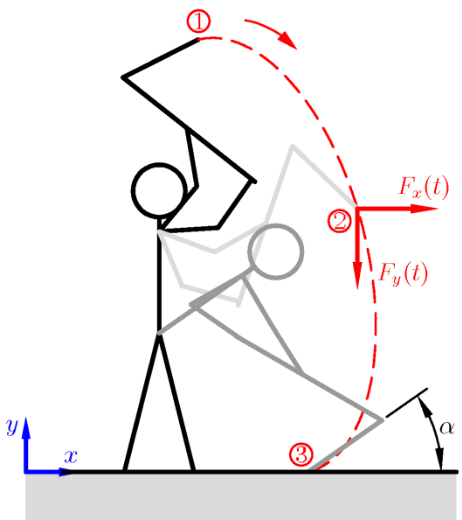

Figure 10: Trajectory for Movement of the Tool Tip and Reaction Forces F_x and F_y.

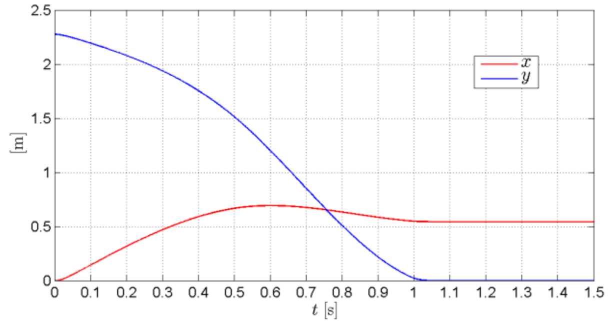

Figure 11: x- and y-Coordinates Over Time for an Example Trajectory.

Using the so defined trajectory as well as geometry and mass data for shaft and tip of the pick, a rigid body model can be set up in MATLAB/SimMechanics, which simulates the movement and provides for example reaction forces (F_x, F_y) on the tool tip as a result, like seen in figure 12.

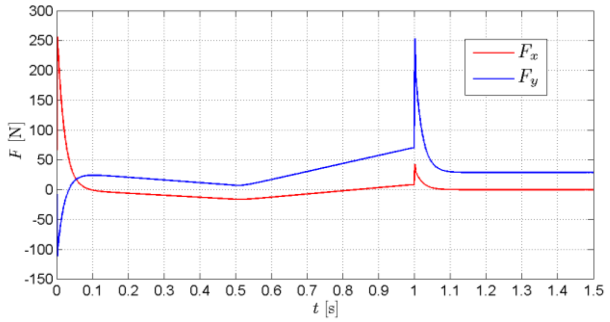

Figure 12: Reaction Forces in x- and y-Direction on the Tool Tip as a Simulation Result for an Example Scenario. At $t = 1$ s, the Impact on the Ground Occurs, Leading to a Peak in the Vertical Force.

In the presented example, salt is mined on the floor, which seems to be rather uncomfortable and unfavorable for body movement and energy requirement. Therefore, future work will investigate mining the salt on vertical surfaces.

4. WOODCHIP FLAME, LIGHTING AND AIR CONSUMPTION

During mining, burning sticks of wood served as the only illumination in the mining halls. Burnt down woodchips were found during excavation in large quantities (Reschreiter et al. 2009).

The resulting light intensity depending on the number of burning woodchips is estimated using a uniform arrangement shown in figure 13. The flame of a burning woodchip is comparable to a flame of a burning candle, therefore we assume a light intensity for each flame of

$$I_v = 1 \text{ cd}. \tag{14}$$

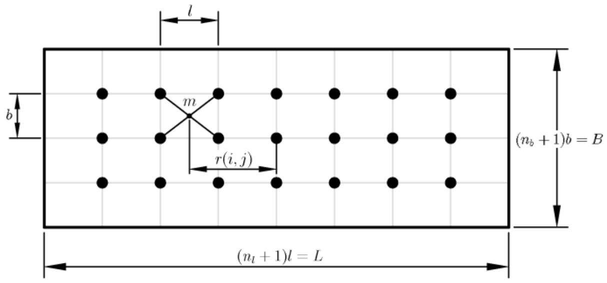

Figure 13: Uniform Arrangement of Burning Woodchips (n_l in Length, n_b in Width) in a Rectangular Mining Hall.

Local minimum illumination occurs at points of maximum distance to the light sources (for example point m in figure 13). For such a point, the distance $r(i,j)$ to each woodchip can be calculated

$$r(i,j) = \sqrt{((i-1)l + \tfrac{l}{2})^2 + ((j-1)b + \tfrac{b}{2})^2} \tag{15}$$

and the sum over all positions leads to the illuminance

$$E_{v,m} = \sum_{i=1}^{n_l} \sum_{j=1}^{n_b} \frac{I_v}{r(i,j)^2}. \tag{16}$$

For different density of woodchips in length and width,

$$\rho_l = \frac{n_l}{L}, \quad \rho_b = \frac{n_b}{B}, \tag{17}$$

calculation results are shown in figure 14.

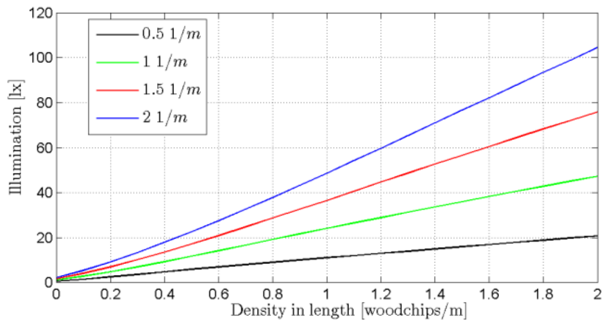

Figure 14: Calculation Results for Illumination for Different Density of Woodchips in Length and Width.

Furthermore, some static calculations are done regarding the oxygen consumption of the flames, which in addition to the oxygen demand of the workers gives information about the necessary air ventilation. For the air consumption of a person doing heavy labour, we assume

$$A_p = 0.81 \ \frac{\text{m}^3}{\text{h}} \tag{18}$$

at 21% percentage of oxygen in the air. A typical woodchip made of fir wood consumes about

$$A_w = 0.014 \text{ m}^3 \tag{19}$$

of oxygen during burning. Altogether, this data leads to the following formula for the total air consumption:

$$A_{\text{total}} = kA_p + n\frac{A_w}{21\% \cdot T}$$

with the number of workers k, total number of woodchips n ($n = n_l \cdot n_b$) and burning time T of a woodchip. Figure 15 depicts some calculation results.

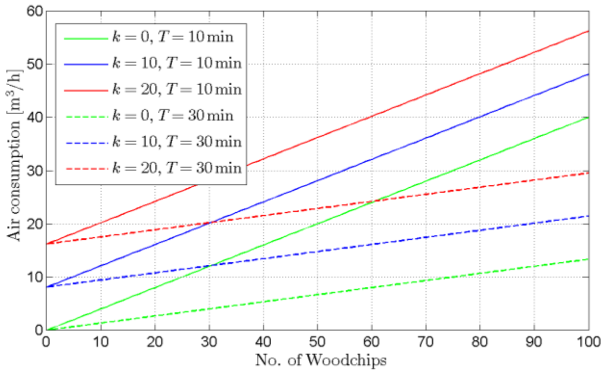

Figure 15: Calculation Results for Air Consumption for Different Number of Woodchips, Burning Time T and Number of Workers k.

This air consumption represents the minimum necessary air exchange in the mining halls in order to keep the oxygen level constant. Taking into account limitations regarding possible air exchange as well as necessary illumination (and therefore necessary number of woodchips), these results also provide reference values for maximum number of workers allowed in the mining halls.

5. CONCLUSION

The calculations and simulation results are visualized graphically. Their evaluations help archaeologists gain knowledge about transport mechanisms and working conditions in the prehistoric salt mines in Hallstatt.

For teaching, these modeling case studies present interesting insights of basic mechanical dynamics including equilibrium of forces, friction or momentum.

In addition, model implementations, which are done in MATLAB, will be included into the MMT system, an e-learning environment for teaching modelling and simulation developed at the Vienna University of Technology (Hafner et al. 2012, Körner et al. 2011).

REFERENCES

Grabner, M., Reschreiter, H., Barth, F.E., Klein, A., Geihofer, D. and Wimmer, R., 2006. Die Dendrochronologie in Hallstatt. *Archäologie Österreichs*, 17(1): 49-58.

Hafner, I., Bicher, M., Winkler, S., Fitsch, U., 2012. MMT – An E-Learning System Based on Computer Numeric System for Teaching Mathematics and Modelling. *In Proceedings of the 7th Vienna Conference on Mathematical Modelling*. February 15-17, 2012, Vienna.

Körner, A., Hafner, I., Bicher, M., Winkler, S., Breitenecker, F., 2011. MMT – A Web Environment for Education in Mathematical Modelling and Simulation. *In Proceedings of ASIM 2011, 21. Symposium Simulationstechnik.* September 7-9, 2011, Winterthur, Switzerland.

Kowarik, K., Reschreiter, H., Wurzer, G., 2012. Modelling Prehistoric Mining. *In Proceedings of the 7th Vienna Conference on Mathematical Modelling*. February 15-17, 2012, Vienna.

Reschreiter, H., Kowarik, K., 2009. The Bronze Age. In: Kern et al. *Kingdom of Salt: 7000 Years of Hallstatt.* Vienna: VPA3, Natural History Museum Vienna, 48-64.